Macromolecules 1993, *26*, 545–550

Comparison of the Mesogenic Properties of Monomeric, Dimeric, and Side-Chain Polymeric Liquid Crystals

C. T. Imrie[†] and F. E. Karasz[*]

Department of Polymer Science and Engineering, University of Massachusetts, Amherst, Massachusetts 01003

G. S. Attard

Department of Chemistry, University of Southampton, Southampton SO9 5NH, England

Received June 20, 1992; Revised Manuscript Received October 26, 1992

ABSTRACT: A new series of homologous side-chain liquid-crystalline polymers based on a polystyrene backbone has been prepared, the poly[[4-[[α-[(4-nitrophenyl)azo]phenyl-4'-oxy]-ω-alkyl]oxy]styrene]s. The thermal properties of these polymers have been studied, and it is shown that all members of the series exhibit a smectic phase. The thermal properties of the polymers are compared with those of the analogous monomers, the 4-(alkyloxy)-4'-nitroazobenzenes, and of the dimers, the α,ω-bis(4-nitroazobenzene-4'-oxy)alkanes. It is found that both the clearing temperatures and the magnitude of the odd–even effect of the polymers lie between those of the monomers and dimers. We rationalize this behavior in terms of a virtual trimer model in which the backbone plays an integral role in determining the mesogenic characteristics of the polymer.

Introduction

Atactic side-chain liquid crystal polymers are an important class of materials with considerable application potential in advanced electro-optic technologies. This arises from a unique duality of properties, namely, glassy behavior coupled with the electro-optic characteristics of low molar mass mesogens.[1] In addition, side-chain liquid crystal polymers are of fundamental interest because the polymer entropy would appear to be antagonistic to the mesogenic order.

There are essentially three components to a side-chain polymer: the backbone, a flexible alkyl spacer, and a semirigid anisometric or mesogenic group. To rationalize the behavior of these materials at the molecular level, a concept that has achieved considerable popularity is the "spacer decoupling" model.[2] The model is based on the assumption that the spacer can decouple the motions and orientational interactions of the mesogenic group from those of the backbone and hence permit liquid-crystalline behavior to be observed. This model, however, fails to adequately explain several characteristic features of these systems. The most notable failure of the model is its inability to explain the experimentally observed increase in the clearing temperature that occurs when a mesogenic monomer is attached to an atactic polymer backbone. Similarly, the spacer decoupling model cannot explain the observation that increasing backbone flexibility for polymers, whose properties lie outside the molecular weight dependent regime, leads to a marked increase in the transition temperatures while having a much smaller effect on the transitional entropies.[2,3]

We have recently presented a molecular field model applicable to side-chain polymers[4] in an attempt to highlight the physics that underlies the formation of liquid-crystalline phases in these systems. The model shows clearly that it is unrealistic to consider the mesogenic group as being decoupled from the backbone. According to this concept, decoupling only occurs in the sense that as the spacer group is increased in length there are a greater number of conformations that can be accessed.[4] This led us to propose recently a new molecular model with which to rationalize the behavior of side-chain polymers, the virtual trimer model, in which for the first time a section of the backbone is considered to be an integral part of the mesogenic species.[3] In that work we noted the similarity in behavior of side-chain liquid crystal polymers and dimeric liquid crystals. To investigate this concept further, we have prepared a series of poly[[4-[[α-[(4-nitrophenyl)azo]phenyl-4'-oxy]-ω-alkyl]oxy]styrene]s (1). In this paper we compare the properties of these polymers with those of the analogous dimers, the α,ω-bis(4-nitroazobenzene-4'-oxy)alkanes[5] (2) and with the analogous monomeric compounds, the 4-(alkyloxy)-4'-nitroazobenzenes (3).

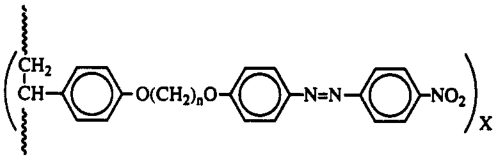

1

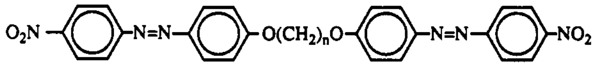

2

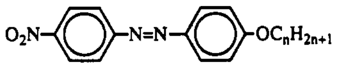

3

We should note that aside from the possible fundamental interest of these polymers they also have application potential as prototype materials in nonlinear optics[6] and in information storage devices[7,8] whose operation relies upon the cis–trans isomerization of the azo linkage. The specific properties of the butyl,[9,10] hexyl,[11] and octyl[12] homologues of the polymer series have been described elsewhere.

Experimental Section

Synthesis. The low molar mass and polymeric liquid crystals were prepared using the sequence of reactions shown in Scheme I.

---

[*] To whom correspondence should be addressed.

[†] Present address: Department of Chemistry, University of Aberdeen, Meston Walk, Old Aberdeen AB9 2UE, Scotland.

0024-9297/93/2226-0545$04.00/0

Scheme I

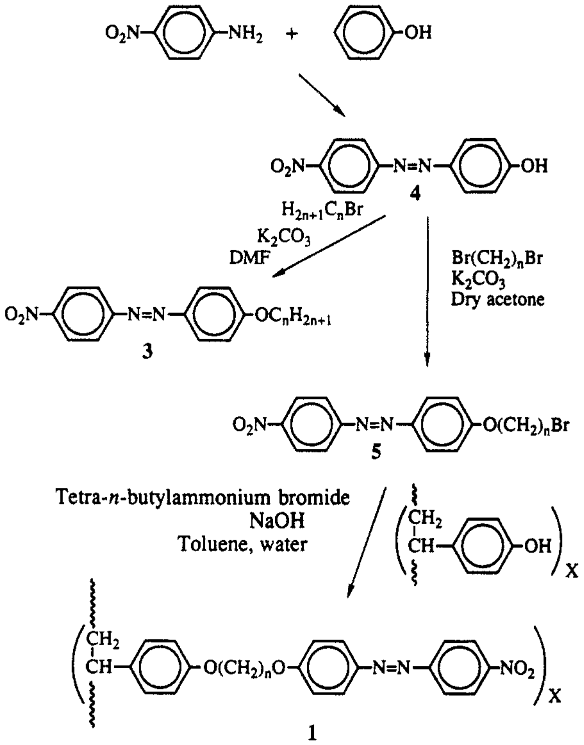

4-Hydroxy-4′-nitroazobenzene (4). The coupling of phenol with diazotized 4-nitroaniline is described in detail elsewhere.[13]

4-(Alkyloxy)-4′-nitroazobenzenes (3). 4-Hydroxy-4′-nitroazobenzene was reacted with a slight excess of a bromoalkane in *N,N*-dimethylformamide (DMF) using potassium carbonate as base. The reaction mixture was refluxed for 3 h, allowed to cool, and then poured into cold water. The resulting orange precipitate was filtered off, washed thoroughly with water, and recrystallized several times from either methanol or ethanol. The yields of bright orange crystals were approximately 70%. The elemental analyses are listed in Table I.

4-(Nonyloxy)-4′-nitroazobenzene: ^{1}H NMR (CDCl$_3$, TMS) δ 8.35 (m, 2 H), 7.97 (m, 4 H), 7.03 (m, 2 H), 4.05 (t, 2 H, OCH$_2$), 1.85 (q, 2 H, OCH$_2$CH_2), 1.50 (q, 2 H, OCH$_2$CH$_2$CH_2), 1.35 (m, 10 H, CH_2), 0.95 (t, 3 H, CH_3); IR (NaCl plate) ν 1344 cm^{-1} (NO stretch); UV–vis (methylene chloride solution) λ_{max} 378 nm.

α-Bromo-ω-(4-nitroazobenzene-4′-oxy)alkanes (5). 4-Hydroxy-4′-nitroazobenzene was reacted with a 10-fold excess of a dibromoalkane using potassium carbonate as base in dry acetone according to the procedure described by Crivello et al.[14] The products were recrystallized from ethanol with hot filtration to ensure the complete removal of any dimeric side product that may have formed during the reaction. The yields were in the range 60–75%, and the elemental analyses are listed in Table II.

1-Bromo-9-(4-nitroazobenzene-4′-oxy)nonane: ^{1}H NMR (CDCl$_3$, TMS) δ 8.35 (m, 2 H), 7.96 (m, 4 H), 7.02 (m, 2 H), 4.06 (t, 2 H, OCH$_2$), 3.42 (t, 2 H, CH$_2$Br), 1.84 (m, 4 H, OCH$_2$CH_2, CH_2CH$_2$Br), 1.47, 1.35 (m, 10 H, CH$_2$); IR (NaCl plate) ν 1344 cm^{-1} (NO stretch); UV–vis (methylene chloride solution) λ_{max} 378 nm.

Polymers (1). The polymers were prepared by the phase-catalyzed reaction of a α-bromo-ω-(4-nitroazobenzene-4′-oxy)alkane with poly(4-hydroxystyrene) (PolySciences; M_w = (9–11) × 10^3) using sodium hydroxide as base and tetra-*n*-butylammonium bromide as the catalyst in a water/toluene system as described in detail elsewhere.[14,15] The reaction was allowed to proceed for 3 days to ensure a complete derivatization of the backbone. The polymer was extracted from the reaction mixture using methylene chloride; the organic extracts were combined and dried. The organic solvents were removed under vacuum. The polymer was redissolved into a small amount of methylene chloride and then precipitated into methanol. The crude polymer was extracted in a Soxhlet apparatus for 48 h using methanol in order to remove unreacted monomer. This was monitored using thin-layer chromatography and verified by elemental analyses; results are listed in Table III. The reaction of the backbone with the brominated mesogenic group was estimated to be 100% complete within our detection limits; we note that IR spectroscopy is a particularly useful tool for this assay.[4] We should note that no appreciable change in the degree of polymerization has been detected during the derivatization process.

Poly[[4-[[1-[(4-nitrophenyl)azo]phenyl-4′-oxy]-9-nonyl]-oxy]styrene]: ^{1}H NMR (CDCl$_3$, TMS) δ 8.30, 7.90 (m, aromatics, 6 H), 6.97, 6.60 (m, aromatics, 6 H), 4.00 (m, OCH$_2$, 4 H), 1.82, 1.45 (m, alkyl, benzylic, 17 H); IR (thin film, NaCl plate) ν 1344 cm^{-1} (NO stretch); UV–vis (methylene chloride solution) λ_{max} 378 nm.

Characterization. The high purity of the final products and their intermediates was verified using thin-layer chromatography. Their structures were confirmed by infrared spectroscopy using an IBM System 9000 FT-IR spectrometer, ^{1}H NMR spectroscopy using a Varian XL200 NMR spectrometer, and elemental analysis performed by the University of Massachusetts Microanalytical Laboratory. The ultraviolet–visible spectra of the materials were recorded using a Perkin-Elmer Lambda 9 UV/vis/near-IR spectrophotometer interfaced to a Perkin-Elmer 7500 laboratory computer.

Thermal Characterization. The phase behavior of the monomers and polymers was investigated using a Carl-Zeiss polarizing microscope equipped with a Linkam hot stage. Further characterization used a Perkin-Elmer DSC-7 differential scanning calorimeter. The transition temperatures quoted are extracted from the calorimetric data obtained for heating scans (10-mg samples; 10 °C min^{-1}) unless otherwise noted.

Results and Discussion

Monomers. The transitional properties of this series are listed in Table IV. All the members of the series exhibit liquid-crystalline behavior, although we should stress that the low members exhibit very monotropic behavior and as a consequence the transition temperatures are difficult to determine. The nematic phases were assigned on the basis of the schlieren optical textures when viewed through the polarizing microscope. On cooling the nematic phases of the hexyl, heptyl, and octyl homologues, the schlieren texture changes to show regions of focal-conic fans, a result implying a layered structure, and homeotropic areas, a result indicating that the director of the phase is perpendicular to the layer planes. As a consequence, the lower temperature phase is assigned as a smectic A phase. A similar texture develops on cooling the isotropic phase of the remaining compounds. We should note that the hexyl, octyl, and decyl homologues of this series have been prepared also by McCulloch and Bailey,[16] and there is good agreement between the two sets of data.

Figure 1 shows the dependence of the transition temperatures on the number *n* of CH$_2$'s in the alkyl segment for the monomeric series. The melting points fall as the chain length is increased for early members of the series; and as *n* is increased further, they exhibit an odd–even alternation. The behavior of the liquid-crystalline transition temperatures is very typical for low molar mass liquid crystals. First the nematic–isotropic transition temperatures exhibit a small alternation on increasing *n*; and second, as *n* is increased, a smectic phase emerges. It should be noted also that the clearing temperature curve becomes rather flat as the chain length is increased, and this result is again typical behavior for mesogens whose transition temperatures are around 100 °C.[17] This observation together with the small odd–even effect in the clearing points will be discussed in detail later. The emergence of smectic properties as the chain length is increased may be thought of as a microphase separation in which the aromatic cores form one domain while the alkyl chains constitute another. There are essentially two driving forces responsible for such a separation; energet-

Table I
Elemental Analyses for the 4-(Alkyloxy)-4′-nitroazobenzenes

n[a]	formula	mol wt	C calc	C found	H calc	H found	N calc	N found
3	$C_{15}H_{15}N_3O_3$	285.3	63.15	62.81	5.30	5.26	14.73	14.73
4	$C_{16}H_{17}N_3O_3$	299.3	64.20	64.28	5.73	5.89	14.04	13.92
5	$C_{17}H_{19}N_3O_3$	313.3	65.16	65.10	6.11	5.91	13.41	13.45
7	$C_{19}H_{23}N_3O_3$	341.4	66.84	67.00	6.79	6.90	12.31	12.40
8	$C_{20}H_{25}N_3O_3$	355.4	67.58	67.51	7.09	6.85	11.82	12.08
9	$C_{21}H_{27}N_3O_3$	369.5	68.27	68.46	7.37	7.50	11.37	11.44
10	$C_{22}H_{29}N_3O_3$	383.5	68.90	68.75	7.62	7.47	10.96	11.15
11	$C_{23}H_{31}N_3O_3$	397.5	69.49	69.80	7.86	7.82	10.57	10.49
12	$C_{24}H_{33}N_3O_3$	411.5	70.04	70.12	8.08	7.75	10.21	10.20

[a] The number of methylene units in the terminal alkyl chain.

Table II
Elemental Analyses for the α-Bromo-ω-(4-nitroazobenzene-4′-oxy)alkanes

n[a]	formula	mol wt	C calc	C found	H calc	H found	N calc	N found
3	$C_{15}H_{14}N_3O_3Br$	364.2	49.47	49.78	3.87	3.88	11.54	11.69
5	$C_{17}H_{18}N_3O_3Br$	392.2	52.05	52.33	4.62	4.61	10.71	10.74
7	$C_{19}H_{22}N_3O_3Br$	420.3	54.29	54.40	5.28	5.27	10.00	9.97
9	$C_{21}H_{26}N_3O_3Br$	448.4	56.25	56.25	5.85	5.88	9.37	9.57
10	$C_{22}H_{28}N_3O_3Br$	462.4	57.14	57.10	6.10	6.06	9.09	9.12
11	$C_{23}H_{30}N_3O_3Br$	476.4	57.98	57.95	6.35	6.35	8.82	8.88
12	$C_{24}H_{32}N_3O_3Br$	490.4	58.77	58.81	6.58	6.51	8.57	8.58

[a] The number of methylene units in the terminal alkyl chains.

Table III
Elemental Analyses for the Polymers

n[a]	repeat unit	mol wt	C calc	C found	H calc	H found	N calc	N found
3	$C_{23}H_{21}N_3O_4$	$(403.4)_m$	68.47	67.54	5.25	5.25	10.42	10.37
5	$C_{25}H_{25}N_3O_4$	$(431.5)_m$	69.59	68.59	5.84	5.48	9.74	9.92
7	$C_{27}H_{29}N_3O_4$	$(459.5)_m$	70.57	69.76	6.36	6.02	9.14	8.83
9	$C_{29}H_{33}N_3O_4$	$(487.6)_m$	71.43	71.12	6.82	6.78	8.62	8.71
10	$C_{30}H_{35}N_3O_4$	$(501.6)_m$	71.80	71.75	7.03	6.96	8.38	8.10
11	$C_{31}H_{37}N_3O_4$	$(515.6)_m$	72.20	71.26	7.23	7.05	8.15	8.25
12	$C_{32}H_{39}N_3O_4$	$(529.6)_m$	72.56	72.25	7.42	7.08	7.93	8.01

[a] The number of methylene units in the alkyl spacer.

Table IV
Transitional Properties of the 4-(Alkyloxy)-4′-nitroazobenzenes

n	$T_{C\text{-}}$/°C	T_{S_AN}/°C	T_{NI}/°C, $^*T_{S_AI}$/°C	$\Delta H_{C\text{-}}$/(J g^{-1})	ΔH_{NI}/(J g^{-1}), $^*\Delta H_{S_AI}$/(J g^{-1})	$\Delta S_{C\text{-}}/R$	$\Delta S_{NI}/R$, $^*\Delta S_{S_AI}/R$
3	132		88^b	100.0		8.4	
4	118		96^b	128.2		11.8	
5	103		93^c	110.3	0.94	11.0	0.10
6	101	$(89)^b$	98^c	123.2	1.02	12.9	0.11
7^a	85	94	97	111.9	1.76	12.8	0.20
8	91	99^b	100	123.2	7.49^d	14.4	0.86^d
9	82		100*	92.5	6.95*	11.5	0.83*
10	89		99*	109.8	7.34*	14.0	0.91*
11	83		100*	120.6	8.26*	16.2	1.06*
12	85		101*	111.1	8.59*	15.3	1.14*

[a] $\Delta H_{S_AN} = 3.96$ J g^{-1}; $\Delta S_{S_AI}/R = 0.44$. [b] Data measured using microscopy. [c] Data measured on cooling scans. [d] Combined S_A–N–I transition.

ically, the mean of the core–core and chain–chain interactions is more favorable than the core–chain interaction and, entropically, the interaction between a core and a chain acts to order the chain and hence is unfavorable, although there are exceptions to this general behavior.[18] The dependence of the clearing entropy on the length of the terminal alkyl chain will be discussed later.

Polymers. The thermal properties of the polymers are listed in Table V. All the members of the series exhibited liquid-crystalline behavior; details of the phase behavior were established using the optical microscope. In order to obtain optical textures from which phase identification was possible, the polymers were heated to approximately 10 °C above their clearing temperature and allowed to cool at 0.2 °C min^{-1} into the mesophase. At the transition, bâtonnets develop and coalesce to form a focal-conic fan texture. In addition, it was possible to achieve homeotropic alignment of the polymers. Thus, using the arguments offered for the monomers, we assigned the phase exhibited by the polymers to smectic A. X-ray diffraction experiments using the butyl[10] and octyl[12] homologues confirm these assignments, revealing specifically the presence of an interdigitated smectic A phase.

The dependence of the transition temperatures on the length of the alkyl spacer in these polymers is shown in Figure 2. The glass transition temperatures decrease as n is increased and exhibit an odd–even effect, with the even-membered homologues having the higher values. The

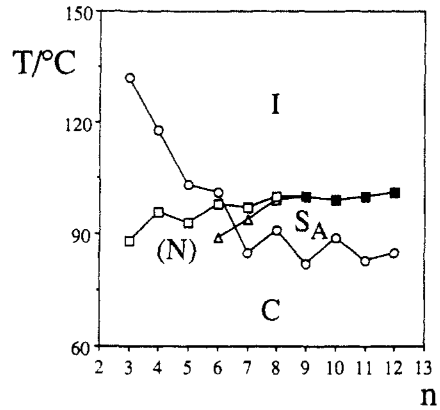

Figure 1. Dependence of the transition temperatures on *n*, the number of methylene units in the terminal alkyl chain of the 4-(alkyloxy)-4′-nitroazobenzenes: ○, melting points; □, nematic–isotropic transitions; △, smectic A–nematic transitions; ■, smectic A–isotropic transitions.

Table V
Thermal Properties of the Polymers

n^a	T_g/°C	T_{CI}/°C	ΔH/(J g^{-1})	$\Delta S/R$
3	72	114	2.60	0.33
4	78	152	4.14	0.49
5	56	148	4.25	0.52
6	55	165	4.84	0.59
7	37	151	5.27	0.69
8	41	162	6.37	0.83
9	26	151	6.69	0.93
10	33	154	7.71	1.09
11	21	140	7.56	1.14
12	18	143	7.52	1.15

[a] The number of methylene units in the alkyl spacer.

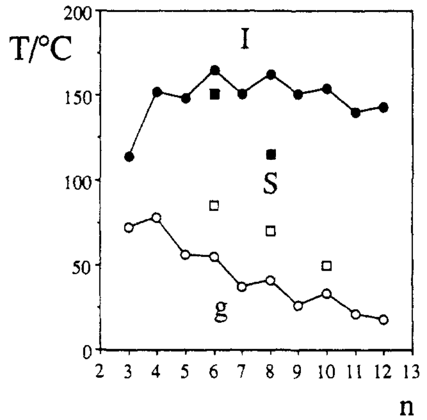

Figure 2. Dependence of the transition temperatures on *n*, the number of methylene units in the alkyl spacer for the polymeric series: glass transitions, ○; smectic–isotropic transitions, ●. Also shown are the glass transitions, □, and the clearing temperatures, ■, for the polymers synthesized by McCulloch and Bailey.[16]

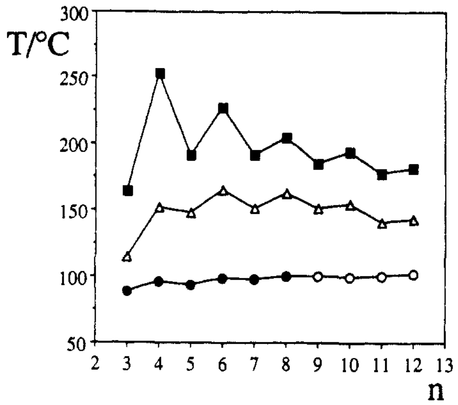

Figure 3. Dependence of the clearing temperatures on *n*, the number of methylene units in the alkyl chain for the polymers (△), the monomers (○ and ●), and the dimers (■). For the monomers, open symbols denote smectic–isotropic transitions and filled symbols represent nematic–isotropic transitions.

decreasing trend in these temperatures is presumably a consequence of the plasticization effect of the side chain on the backbone; the molecular significance of the alternation in the temperatures is, however, unclear. It should be noted, however, that, as the spacer chain length was increased, the heat capacity change associated with the glass transition became increasingly weaker and hence the uncertainty in the T_g's became larger. In some instances the magnitude of this error approaches the size of the alternation in the measured temperatures. Other homologous series of polystyrene-based liquid crystal polymers also appear to exhibit an odd–even effect in their glass transition temperatures.[3,15] The smectic–isotropic transition temperatures also show an odd–even effect as *n* is increased, again with the even members having the higher values; we will return to this observation later.

McCulloch and Bailey[16] have reported some thermal properties of the hexyl, octyl, and decyl homologues of the polymer series, and their data are also shown in Figure 2. It can be seen that the agreement between the two sets of data is poor. The glass transition temperatures of their polymers are approximately 30 °C higher than those we report, whereas the clearing temperatures are considerably lower. Indeed, for the decyl member they report an amorphous polymer without mesogenic phases, whereas the material described here has a clearing temperature of 154 °C. There are two possible explanations for these large differences. First, McCulloch and Bailey describe two synthetic routes to obtain the polymers; one of these is essentially identical to that we use, whereas the second method involves reacting the monomer with poly(4-hydroxystyrene) in DMF using potassium carbonate as base. This latter method appears to result in incomplete reaction of the mesogen with the backbone, but the authors do not state which method was used to prepare which polymers. Incomplete derivatization of the backbone would certainly account for the higher glass transition temperatures and also the lower clearing temperatures. However, it should be noted that, particularly for the octyl and decyl members, the level of derivatization must be low to account for the large decreases in T_{CI} of the resulting copolymers. In principle, an alternative explanation for these large differences involves the molecular weights of the polymers, but unfortunately no details of the backbone used were provided. Molecular weight effects, however, are probably not responsible for these differences, because it would be difficult to rationalize the very large decrease in the clearing temperatures on passing from the hexyl to the decyl members.

Comparison of the Monomers, Dimers, and Polymers. Figure 3 compares the clearing temperatures for the monomeric, dimeric, and polymeric series. The side-chain polymers have clearing temperatures intermediate between those of the monomers and dimers. It is important to note also that the magnitude of the alternation exhibited by the clearing temperatures on increasing the length of the alkyl chain increases in the order dimer > polymer > monomer. If we first consider the behavior of the monomers, then, as has already been noted, many conventional monomeric mesogens with clearing temperatures in the region of 100 °C tend to display rather flat clearing temperature curves.[17] If, however, the clearing temperatures are below 100 °C, then the clearing temperature curve tends to rise with a larger odd–even effect super-

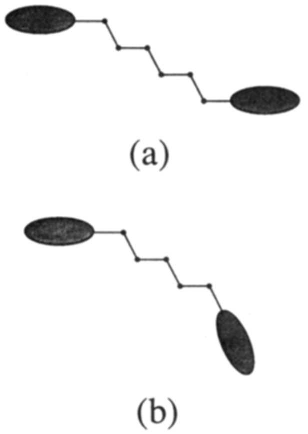

Figure 4. Schematic representations of the all-trans conformations of (a) an even-membered and (b) an odd-membered dimeric liquid crystal.

imposed on it, whereas if the transition temperatures are in excess of 100 °C, then the clearing temperatures tend to fall with little or no alternation. This behavior can be rationalized by considering the dual effects of increasing the length of a terminal alkyl chain.[19] First, increasing the length of the chain increases the molecular anisometry and hence increases the clearing temperature. However, increasing the length of the chain serves also to dilute the core–core interactions, thereby depressing the clearing temperature. The role of the terminal chain in determining the clearing temperature is dependent on the interaction strength of the cores. For large cores—for example, three-ring systems—the presence of the chain serves merely to dilute the core–core interactions; thus, the clearing temperatures fall with little or no alternation. In contrast, for small cores—for example, two-ring systems—the increased molecular anisometry dominates, and increasing transition temperatures are observed with a much larger odd–even effect. For intermediate strength interaction parameters, the two effects balance, and rather flat curves are observed; experimentally, this is found to be the case for systems with clearing temperatures in the region of 100 °C. This molecular interpretation allows for the behavior of laterally as well as terminally attached chains[19,20] and has been formalized using molecular field theory.[21]

In the case of the dimers, we see generally far higher transition temperatures and a pronounced odd–even effect. The higher transition temperatures can be attributed to the presence of the second mesogenic group, which greatly increases the molecular anisometry, whereas the pronounced odd–even effect arises from the substantial change in molecular shape on increasing the length of the flexible spacer. For an even-membered spacer, the two mesogenic groups can be coparallel in the all-trans conformation, whereas for an odd-membered spacer, they subtend an angle of approximately 108° (see Figure 4).

We turn our attention now to the side-chain polymers. If we first attempt to explain their observed behavior in terms of the conventional concept of the spacer chain affecting a decoupling of the mesogenic groups from the polymer backbone, then it is very difficult to adequately account for either the enhanced transition temperatures or their larger alternation on varying the spacer chain length. Indeed, as was noted in the Introduction, molecular field theory[4] clearly shows that the orientational order of the mesogenic groups and the conformational statistics of the spacer chain and polymer backbone are interrelated. This theoretical treatment led us to propose the "virtual trimer" model with which to interpret the stabilization of mesophases in side-chain polymers.[3] We consider a virtual trimer to consist of three different types of structural units; two mesogenic groups, two spacers, and a section of the polymer chain (shown schematically in Figure 5). From this model, it is apparent that the presence of the second mesogenic unit in the virtual trimer can account for the rise in transition temperatures on attaching the monomer to the polymer. It can also account for the increased alternation in the clearing temperatures, for the spacers to some extent affect the relative orientations of the mesogenic units. It should be noted, however, that this is a smaller effect than that seen in dimers, because the 1,3-disubstituted polymer chain ensures that the overall structure is always nonlinear. The properties of the polymers will, therefore, approach those of the odd-membered dimers or trimers. In contrast, 1,4-disubstituted polymers have the potential of exhibiting more elongated virtual trimers, and their properties should approach those of even-membered dimers. This possibility is one design implication of the model we are currently exploring. It may be noted that the overall lengths of the dimers synthesized are considerably lower than those of the virtual trimers.

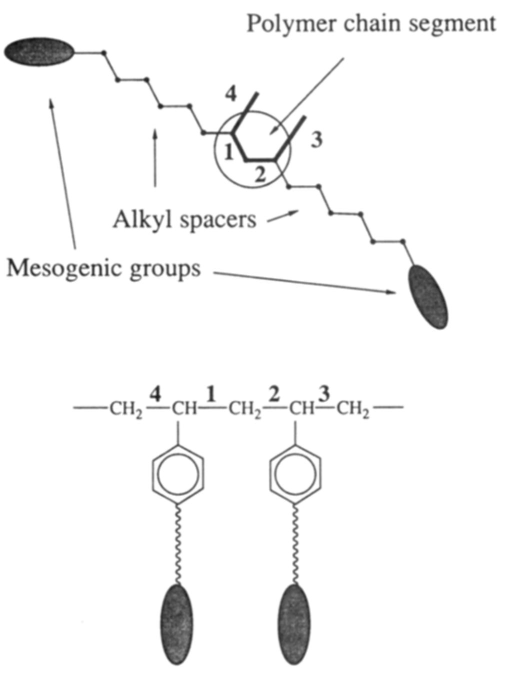

Figure 5. Schematic representation of a virtual trimer.

Figure 6 compares the dependence of the clearing entropies, expressed as the dimensionless quantities $\Delta S/R$, on the length of the alkyl chains for the monomer, dimer, and polymer series. The monomers exhibit very low $\Delta S/R$ values for the nematic–isotropic transition, but these values increase sharply on passing to smectic–isotropic transitions. The general trend for the monomers is an increasing one with little or no alternation, and this behavior is very typical.[18] The corresponding polymers exhibit higher $\Delta S/R$ values than do the monomers, although this difference diminishes as the alkyl chain length increases. The dimers exhibit very different behavior; the entropies of transition show a large alternation as the length of the spacer is increased. Underlying this alternation is the difference in the long-range orientational order between odd- and even-membered dimers at the clearing point.[18] It should be noted that the transition entropies for this particular dimeric series are anomalously low, as are the clearing temperatures, and this finding was attributed to the thermally activated cis–trans isomerization of the azo

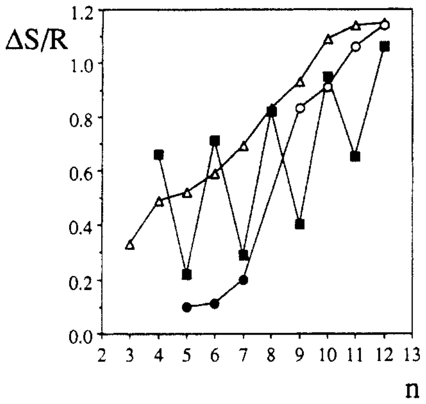

Figure 6. Dependence of the clearing entropies on *n*, the number of methylene units in the alkyl chain for the polymers (△), the monomers (○ and ●), and the dimers (■). For the monomers, open symbols denote smectic–isotropic transitions and filled symbols represent nematic–isotropic transitions.

linkage.[5] Thus, at elevated temperatures there is a greater concentration of the cis-isomer, which reduces the anisometric shape of the group, thereby decreasing the clearing temperature and entropy.[5] We should stress that the polymers do not exhibit this very large alternation because the overall shape of the virtual trimer is nonlinear; therefore, it resembles an odd-membered dimer.

There are relatively few examples of side-chain polymers containing nitroazobenzene as the mesogenic group. Noël et al.[22] reported copolymers containing the nitroazobenzene moiety as prototype materials for nonlinear optic applications. Lorenz[23] prepared four polymethacrylates containing nitroazobenzene as the mesogenic group substituents. The hexyl and octyl homologues of this series show glass transition temperatures similar to those of the analogous polystyrene homologues, whereas T_g for the propyl homologue is about 23 °C higher; the undecyl homologue forms a semicrystalline phase. The clearing temperatures of the hexyl and octyl homologues of the polymethacrylate series are slightly higher than those of the polystyrene analogues, whereas the propyl homologue exhibits a clearing temperature about 44 °C higher, and the undecyl member has a clearing temperature 25 °C greater. The behavior of the hexyl and octyl members of the polymethacrylate series is in accord with the anticipated effect of increasing the flexibility of the polymer chain.[3] In contrast, the properties of the propyl and undecyl are difficult to rationalize. It is interesting to note that these polymers are prepared by free-radical polymerization even though the nitro group is normally considered to be an inhibitor of such reactions.

Conclusions

The thermal properties of side-chain liquid crystal polymers are intermediate between those of the corresponding monomeric and dimeric liquid crystals. We have rationalized this behavior in terms of a new molecular model, the virtual trimer model. Further speculation must await the results from model calculations as well as the preparation of realistic model trimeric compounds.

Acknowledgment. We are pleased to acknowledge support from AFOSR Contract F49620-87-C-0111.

References and Notes

(1) Attard, G. S. In *High Value Polymers*; Fawcett, A. H., Ed.; Royal Society of Chemistry: London, 1991; p 131.
(2) For a discussion of the spacer decoupling model and its limitations, see: Percec, V.; Pugh, C. In *Side Chain Liquid Crystal Polymers*; McArdle, C. B., Ed.; Blackie and Sons: Glasgow, U.K., 1989; Chapter 3.
(3) Imrie, C. T.; Karasz, F. E.; Attard, G. S., submitted to *Macromolecules*.
(4) Attard, G. S.; Dave, J. S.; Wallington, A.; Imrie, C. T.; Karasz, F. E. *Makromol. Chem.* **1991**, *192*, 1495.
(5) Attard, G. S.; Garnett, S.; Hickman, C. G.; Imrie, C. T.; Taylor, L. *Liq. Cryst.* **1990**, *7*, 495.
(6) Möhlmann, G. R.; van der Vorst, C. P. J. M. In *Side Chain Liquid Crystal Polymers*; McArdle, C. B., Ed.; Blackie and Sons: Glasgow, U.K., 1989; Chapter 12.
(7) Eich, M.; Wendorff, J. *Makromol. Chem., Rapid Commun.* **1987**, *8*, 467.
(8) Eich, M.; Wendorff, J.; Ringsdorf, H.; Schmidt, H. W. *Makromol. Chem.* **1985**, *186*, 2639.
(9) Attard, G. S.; Karasz, F. E. *Makromol. Chem., Rapid Commun.* **1990**, *11*, 145.
(10) Imrie, C. T.; Schleeh, T.; Karasz, F. E.; Attard, G. S. *Macromolecules* **1993**, *26*, 539.
(11) Imrie, C. T.; Karasz, F. E.; Attard, G. S. *Liq. Cryst.* **1991**, *9*, 47.
(12) Schleeh, T.; Imrie, C. T.; Rice, D.; Karasz, F. E.; Attard, G. S. *J. Polym. Sci. A.*, in press.
(13) *Vogel's Textbook of Practical Organic Chemistry*, 4th ed.; Furniss, B. S., Hannaford, A. J., Rogers, V., Smith, P. W. G., Tatchell, A. R., Revisors; Longman Scientific and Technical: New York, 1987.
(14) Crivello, J. V.; Deptolla, M.; Ringsdorf, H. *Liq. Cryst.* **1988**, *3*, 235.
(15) Imrie, C. T.; Karasz, F. E.; Attard, G. S. *Macromolecules* **1992**, *25*, 1278.
(16) McCulloch, I. A.; Bailey, R. T. In *Nonlinear Optical Properties of Organic Materials II*; Khanarian, G., Ed.; SPIE: San Diego, 1989; Vol. 1147, pp 134–140.
(17) Gray, G. W. In *The Molecular Physics of Liquid Crystals*; Luckhurst, G. R., Gray, G. W., Eds.; Academic Press: New York, 1979; Chapter 1.
(18) Date, R. W.; Imrie, C. T.; Luckhurst, G. R.; Seddon, J. M. *Liq. Cryst.* **1992**, *12*, 203.
(19) Imrie, C. T.; Taylor, L. *Liq. Cryst.* **1989**, *6*, 1.
(20) Attard, G. S.; Imrie, C. T. *Liq. Cryst.* **1989**, *6*, 387.
(21) Emerson, A. P. J. Ph.D. Dissertation, University of Southampton, Southampton, England, 1991.
(22) Noël, C.; Friedrich, C.; Leonard, V.; Le Barny, P.; Ravaux, G.; Dubois, J. C. *Makromol. Chem., Macromol. Symp.* **1989**, *24*, 283.
(23) Lorenz, R. *Liq. Cryst.* **1991**, *9*, 127.